Engineering Axial Resolution Realtime and Post-Recording of Incoherent Holograms Using Hybridization Techniques

Shivasubramanian Gopinath,[a*] Aravind Simon John Francis Rajeswary,[a] Vijayakumar Anand[a,b]
[a]Institute of Physics, University of Tartu, W. Ostwaldi 1, 50411 Tartu, Estonia
[b]Optical Sciences Center and ARC Training Centre in Surface Engineering for Advanced Materials (SEAM), Swinburne University of Technology, Australia
*shivasubramanian.gopinath@ut.ee

ABSTRACT

In incoherent digital holography (IDH) and in any imaging technique, the lateral and axial resolutions are intertwined and consequently changing one characteristic affects the other. In this study, we present two new hybridization techniques HM-1, and HM-2 for IDH, one for real-time and another for post-recording of holograms respectively, to engineer the axial resolution independent of lateral resolution. Two optical functions namely a lens and an axicon, with a low focal depth and a high focal depth respectively are considered. In both hybridization techniques, the axial resolution can be tuned between the limits of the axial resolutions of lens and axicon, while maintaining a constant lateral resolution. In HM-1, the axial resolution was engineered using a special phase mask designed using a modified version of Gerchberg-Saxton algorithm that can generate a spherical beam and Bessel beam for every object point and create self-interference between them. By controlling the strengths of the two beams, the axial resolution can be tuned without changing the lateral resolution. This method requires an active optical device such as a spatial light modulator. HM-2 involves two recordings of the same scene, one with a lens and another with an axicon which are then combined after recording. By controlling the weights of the two recordings, the axial resolution can be tuned between the limits of lens and the axicon independent of lateral resolution. In this case, passive diffractive or refractive optical elements are sufficient. Both hybridization techniques are implemented in indirect imaging mode consisting of three steps: recording point spread hologram, object hologram and reconstruction by Lucy-Richardson-Rosen algorithm.

Keywords: incoherent digital holography, axial resolution, hybridization, Lucy-Richardson-Rosen algorithm, computational imaging.

1. INTRODUCTION

Imaging technologies occupy a significant place in everyone's life. New imaging devices with surprising capabilities are emerging every day to make people's life easier. Most imaging devices available in the market use the direct imaging method, which records the image of an object by a single click directly by a camera. Incoherent digital holography (IDH) is a widely used imaging method in which the image of the object is recorded indirectly i.e., recording object holograms and reconstruction by computational algorithms. There are multiple parameters associated with every image recorded. Among them, two of the most important parameters are the axial resolution (AR) and the lateral resolution (LR), both are interdependent. If LR is changed, then AR is also changed.[1] Axicons have a long focal depth and so they are often employed in the direct imaging approach for capturing objects with a high depth of field. However, the sidelobes in the Bessel beam produced by the axicon extinguishes the high spatial frequencies during imaging.[2,3,4,5] The sidelobes can be eliminated by deconvolution[6] and engineering[7] methods. In indirect imaging mode and in IDH, it is possible to replace manual refocusing as is done in direct imaging methods by computational refocusing in the form of numerical back propagation.[8,9,10] One of the widely used IDH techniques based on self-interference is Fresnel incoherent correlation holography (FINCH).[11,12] In FINCH, randomly multiplexed diffractive lenses are used to obtain the self-interference hologram. To avoid the twin image and bias terms, FINCH requires alteast three camera shots with different phase shifts. FINCH exhibits a lower AR and higher LR when compared to direct imaging systems with the same numerical aperture. Another IDH method called as coded aperture correlation holography (COACH)[13] was developed based on FINCH in 2016. COACH has the same AR and LR as those of direct imaging systems. Hybridization is an important tool used in many research areas, by which blended features are produced which are not naturally present. A new hybridization method was developed by integrating FINCH and COACH which allows to tune LR and AR between the limits of

International Conference on Optical and Photonic Engineering (icOPEN 2023), edited by Haixia Wang, Fang Cheng, Cuong Dang, Aaron Danner, Qian Kemao, Proc. of SPIE Vol. 13069, 130690H
 · 0277-786X · doi: 10.1117/12.3015742

FINCH and COACH.[14] IDH and coded aperture imaging (CAI) were connected by the invention of COACH where the recording process was similar to IDH and the reconstruction method was similar to CAI.[15,16,17,18,19] Later COACH was upgraded to interferenceless COACH (I-COACH), where the hologram was recorded without two-beam interference.[20] In the first version of I-COACH, like FINCH and COACH three camera shots were recorded. Later, in the next version of I-COACH, a new computational reconstruction method called non-linear reconstruction (NLR) was developed which enabled single shot capability in I-COACH.[21] After the development of NLR, another hybridization approach called coded aperture with FINCH intensity responses (CAFIR) was developed for mixing FINCH and COACH such that the AR of COACH and LR of FINCH can be obtained.[22] In another study of I-COACH, the performance was investigated for a wide variety of deterministic and random optical fields and NLR was found not optimal for deterministic optical fields.[23] Based on NLR and the well-known deconvolution method called Lucy-Richardson algorithm (LRA),[24,25] a new computational reconstruction algorithm called Lucy-Richardson-Rosen algorithm (LRRA) was developed.[26] The performance of LRRA was found to be better than NLR and LRA when implementing deterministic optical fields.[27,28,29] Recently, several methods were reported to tune AR independent of LR using Bessel, Airy and self-rotating beams.[30,31,32] In this study, we proposed and demonstrated two hybridization methods HM-1 and HM-2 for engineering AR independent of LR both in real time and post recording. In both methods, two optical elements namely lens and axicon were used and LRRA was used for image reconstruction. In HM-1, the hybrid phase masks are designed by combining lens and axicon to generate spherical and Bessel beams and create self-interference. In HM-1, the AR can be engineered in real time between the limits of the lens and axicon by controlling the strengths of the two beams. In HM-2, two camera shots of the same scene are recorded collinearly using passive refractive lens and axicon. The AR can be engineered after recording by applying different weights to the recorded holograms. The rest of the manuscript consists of methodology, simulation studies, experiments and conclusion and summary.

2. METHODOLOGY

The concept figures of HM-1 and HM-2 are shown in Fig. 1a and Fig. 1b respectively. In HM-1, two diffractive optical functions namely lens and axicon are chosen. The weights of the two optical functions are controlled by variables T_1 and T_2. When ($T_1 = 1$; $T_2 = 0$), the phase mask is pure and it behaves as a lens and when ($T_1 = 0$; $T_2 = 1$) again the phase mask is pure and it behaves as an axicon. Between the above two limits, the phase mask is hybrid containing the functions of both lens and an axicon. However, it is impossible to create a pure phase function that can be displayed on a spatial light modulator (SLM) by combining two pure phase functions as the result of combining two pure phase function is a complex function. To combine two pure phase functions for displaying on the SLM, random multiplexing is usually used which results in scattering noises.[11,30,31,32] Recently, a novel computational method called transport of amplitude into phase based on Gerchberg-Saxton algorithm (TAP-GSA) was developed for multiplexing two pure phase functions into a pure phase function without random multiplexing.[33,34] In this study, TAP-GSA has been used for combining two pure phase functions. The light emitted from an object point enters the SLM. For non-hybrid cases such as lens and axicon, since a single beam is generated, the system acts similar to CAI and I-COACH. When the hybrid pure phase mask generated from the TAP-GSA algorithm was displayed, multiple beams are generated at the SLM and self-interference is created like FINCH or COACH. In the first step, a point object was used to record the point spread function (PSF) at two depths. In the next step, two different objects are used to record the object intensity distribution (OID), similarly at two depths and then they are combined into a single matrix. The 3D information of the object is reconstructed by cross correlating the PSF and OID by LRRA as shown in Fig. 2. This allows to engineer AR in real time. In HM-2, two passive refractive optical elements namely lens and axicon are used and the PSF and OID are recorded collinearly at the same time by two image sensors. The recording process is then repeated for another depth. As per requirement, the hybrid PSF is created by summing the recorded PSF of lens and axicon after applying different weights. Same procedure is followed to create hybrid OID. The object is reconstructed by LRRA. By implementing's HM-2, it is possible to engineer AR independent of LR after recording.

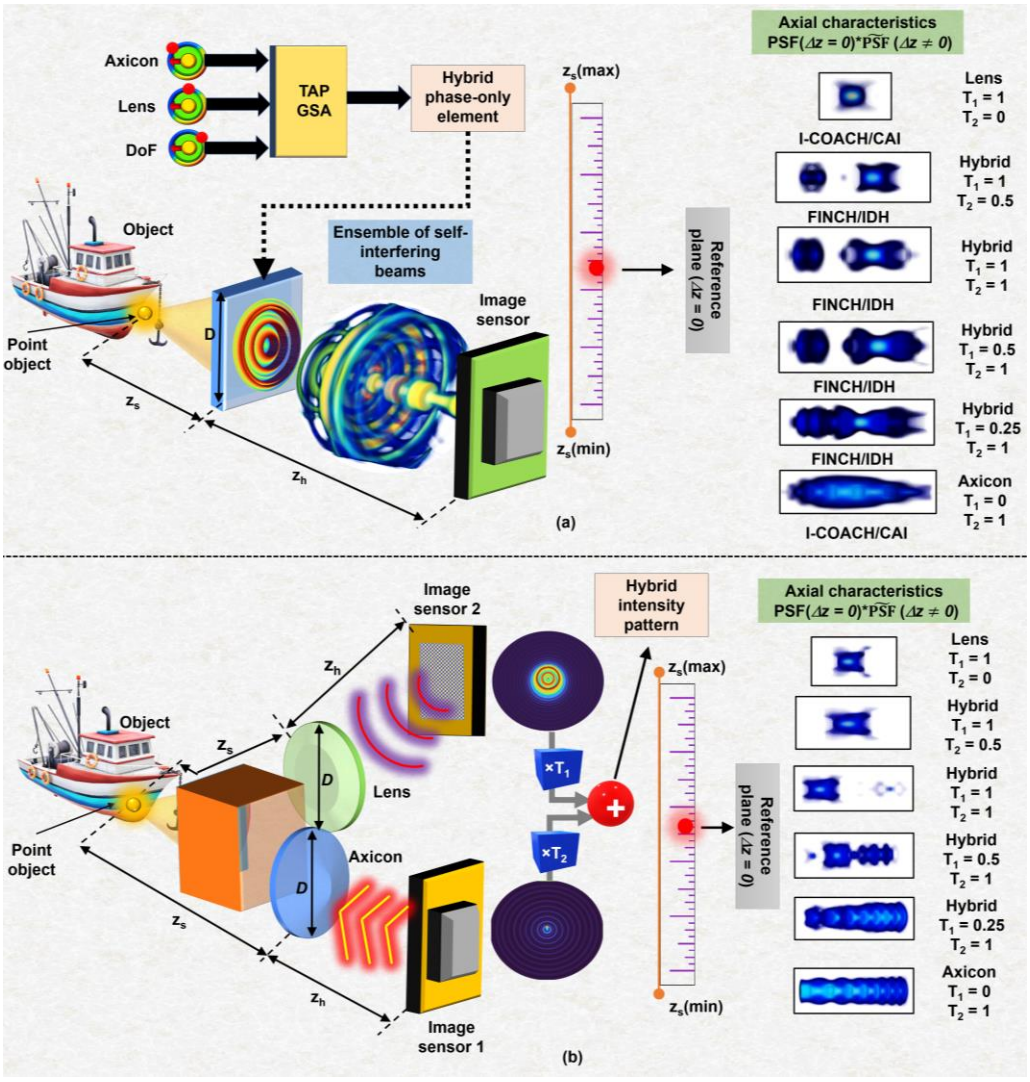

Figure 1. Concept figures of (a) HM-1, (b) HM-2. The object and recording distances are denoted as z_s and z_h.

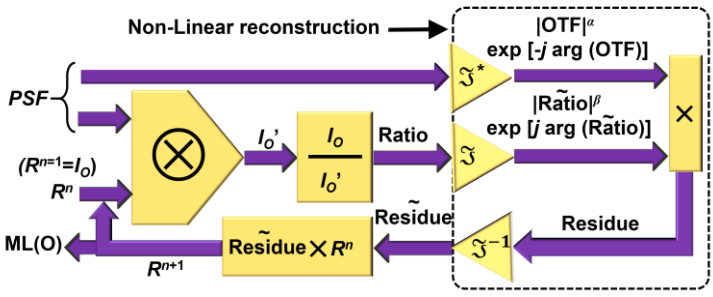

Figure 2. Schematic of LRRA. PSF – point spread function; I_O – object intensity distribution; n – number of iterations; ML – maximum likelihood; OTF – optical transfer function; ⊗ - 2D convolutional operator; $\Im$ - Fourier transform; * - complex conjugate, $^{-1}$ – inverse; R^{n+1} – $(n+1)^{th}$ solution. The parameters α and β are tuned between -1 to +1 to obtain the optimal solution with minimum n.

3. SIMULATION STUDIES

The simulation studies were carried out using MATLAB. A matrix size of 500 × 500 pixels, pixel size Δ = 8 μm, wavelength λ = 632.8 nm, and z_h = 30 cm were used. The logos of University of Tartu and CIPHR were used as test objects. The simulated PSFs at depths (z_s = 27 cm) and (z_s = 30 cm), OID and reconstruction results by LRRA at depths (z_s = 27 cm) and (z_s = 30 cm) are shown in first, second, third, fourth and fifth columns in Fig. 3 and Fig. 4 for lens, hybrid state and axicon for HM-1 and HM-2 respectively. As seen from the reconstruction results of HM-1 and HM-2, in the case of lens one object is focused and the other object is blurred. In case of axicon, both objects are focused. The AR decreased when we move from lens to axicon through the hybrid states.

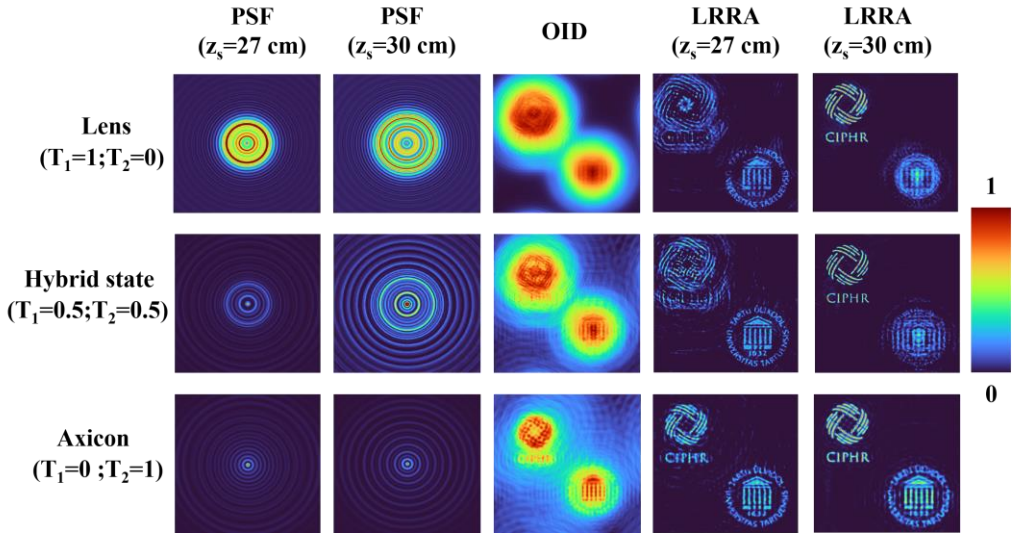

Figure 3. Simulation results of HM-1.

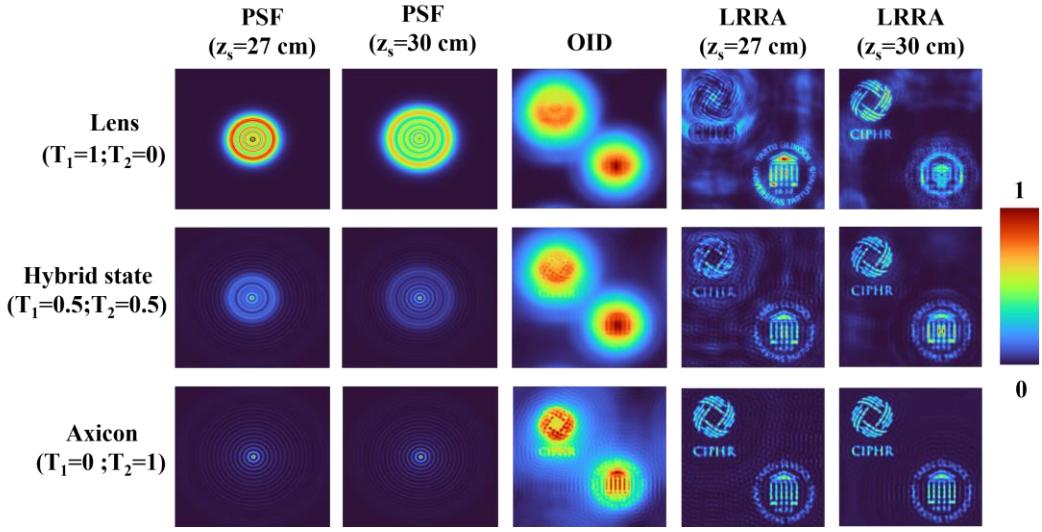

Figure 4. Simulation results of HM-2.

4. EXPERIMENTS

An optical experimental setup was built using the following components: a high-power LED (Thorlabs, 940 mW, λ = 660 nm and $\Delta\lambda$ = 20 nm), refractive lenses, polarizer, USAF object (Group – 5, Element 1 and 3), beam splitter, SLM (Thorlabs Exulus HD2, 1920×1200 pixels, pixel size = 8 μm) and an image sensor (Zelux CS165MU/M 1.6 MP

monochrome CMOS camera, 1440×1080 pixels with pixel size ~3.5 μm). The object is critically illuminated by a refractive lens with a focal length of 5 cm. Another refractive lens with a focal length of 5 cm was used to collimate the light emitted from the object. A polarizer was used to polarize the collimated light along the active axis of the SLM. The polarized light passed through a beam splitter and reached the SLM. On the SLM, the phase masks of lens ($T_1 = 1$; $T_2 = 0$), hybrid state ($T_1 = 0.5$; $T_2 = 0.5$) and axicon ($T_1 = 0$; $T_2 = 1$) were displayed one after the other and the PSFs and OIDs were recorded using the image sensor. The PSFs were recorded using a pinhole with a diameter of 50 μm. The object distance z_s was 5 cm and the recording distance z_h was 17.8 cm. The experiment was repeated for another depth $z_s = 5.6$ cm to demonstrate 3D imaging. The experimental results of HM-1 are shown in Fig. 5: first row shows the phase mask designed by TAP-GSA, second row shows the PSF at depth ($z_s = 5$ cm), third row shows the PSF at depth ($z_s = 5.6$ cm), fourth row shows the summed OID corresponding to both depths ($z_s = 5$ cm) and ($z_s = 5.6$ cm), fifth row shows the reconstruction results by LRRA at depth ($z_s = 5$ cm), and sixth row shows reconstruction results by LRRA at depth ($z_s = 5.6$ cm) of lens, hybrid state and axicon respectively. From the reconstruction results at both depths for a lens it can be seen that one object was focused, and other object was blurred which demonstrates a high AR. In the case of axicon, both objects were perfectly focused which demonstrates a low AR. To engineer the AR in real time, the lens and axicon were combined to create a hybrid state. Depending upon the requirement, hybrid phase masks can be engineered with different strengths of lens and axicon. In this study, the hybrid phase mask was designed by combining lens and axicon with equal strengths i.e., 50% of lens and 50% of axicon. From the reconstruction results for different cases, it can be seen that the blur of the other plane gradually decreases when we move from lens to axicon. The HM-2 allows to engineer the AR after completing the recording process. In order to do that, the recorded PSF of lens and axicon are combined by applying different weights to the recorded holograms and the hybrid PSF is created. The same process is repeated for the OID. The experimental results of HM-2 are shown in Fig. 6: first row shows the PSF at depth ($z_s = 5$ cm), second row shows the PSF at depth ($z_s = 5.6$ cm), third row shows the summed OID corresponding to both depths ($z_s = 5$ cm) and ($z_s = 5.6$ cm), fourth row shows the reconstruction results by LRRA at depth ($z_s = 5$ cm), and similarly the fifth row shows at depth ($z_s = 5.6$ cm) of lens, hybrid state and axicon respectively. From the reconstruction results, it is seen that AR decreased when we move from lens to axicon.

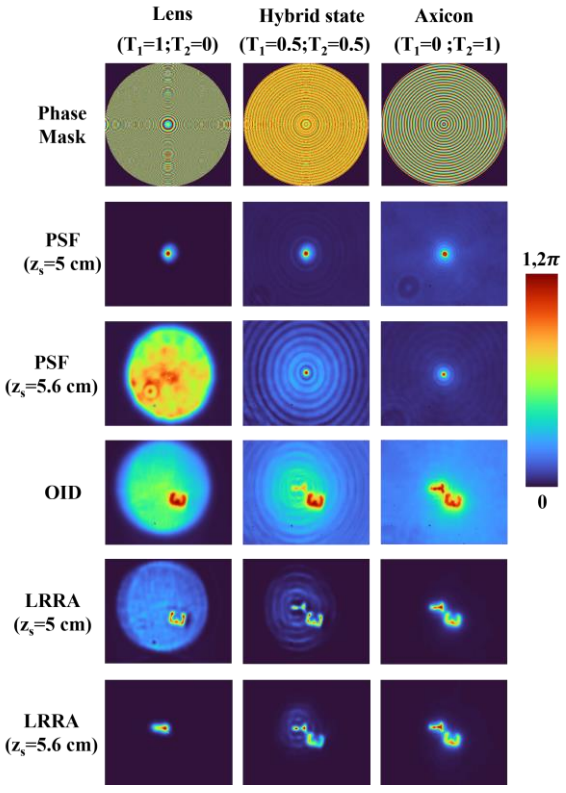

Figure 5. Experimental results of HM-1.

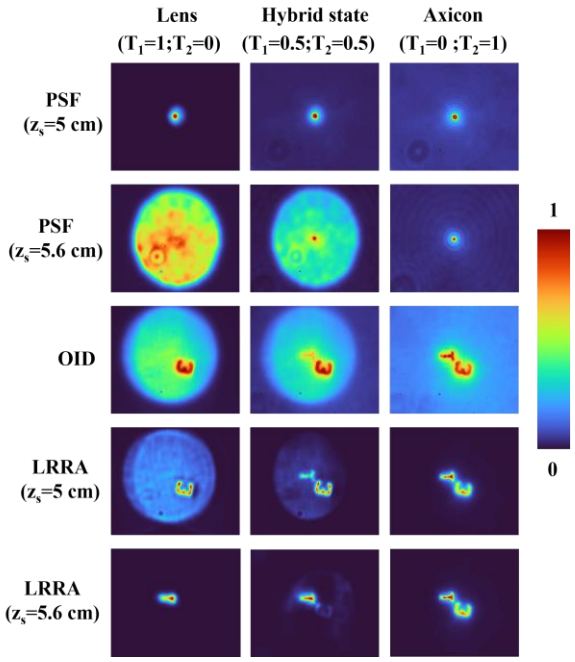

Figure 6. Experimental results of HM-2.

5. SUMMARY AND CONCLUSION

In this study, two novel hybridization methods HM-1 and HM-2 were developed using only two optical functions: lens and axicon to engineer AR independent of LR in real time as well as post recording. The two methods namely HM-1 and HM-2 even though used for two purposes namely real-time AR tuning and AR tuning post recording independent of LR respectively, they are quite similar. Both use same two optical beams and tune the imaging characteristics between the limits of the two beams by controlling the strengths of the two beams during interaction. The fundamental difference between the two methods HM-1 and HM-2 lies in the nature of interaction. In HM-1, the interaction is achieved using a self-interference, whereas in HM-2, the interaction is achieved using an intensity addition. The simulation and experimental results confirm the tunability of AR independent of LR in both methods. We believe that the developed hybridization methods will revolutionize the fields like IDH, microscopy, cinematography, medical imaging etc.

Funding. This research was funded by the European Union's Horizon 2020 research and innovation programme, grant agreement No. 857627 (CIPHR).

REFERENCES

[1] Barrett, H. H. and Myers, K. J., "Foundations of image science," John Wiley & Sons, (2013).
[2] Khonina, S. N., Kazanskiy, N. L., Karpeev, S. V. and Butt, M. A., "Bessel Beam: Significance and Applications—A Progressive Review," Micromachines 11(11), 997 (2020).
[3] Zhai, Z., He, X., Yu, X., Liu, D., Lv, Q., Xiong, Z., Wang, X. and Xu, Z., "Parallel Bessel beam arrays generated by envelope phase holograms," Optics and Lasers in Engineering 161, 107348 (2023).
[4] Vijayakumar, A., Rosen, J. and Juodkazis, S., "Review of engineering techniques in chaotic coded aperture imagers," Light: Advanced Manufacturing 3, 739 (2022).
[5] Indebetouw, G., "Nondiffracting optical fields: some remarks on their analysis and synthesis," Journal of the Optical Society of America A, 6(1), 150-152 (1989).
[6] Smith, D., Ng, S.H., Han, M., Katkus, T., Anand, V., Glazebrook, K. and Juodkazis, S., "Imaging with diffractive axicons rapidly milled on sapphire by femtosecond laser ablation," Appl. Phys. B 127(11), 154 (2021).

[7] Dharmavarapu, R., Bhattacharya, S. and Juodkazis, S., "Diffractive optics for axial intensity shaping of Bessel beams," Journal of Optics 20(8), 085606 (2018).
[8] Rosen, J., Vijayakumar, A., Kumar, M., Rai, M. R., Kelner, R., Kashter, Y., Bulbul, A. and Mukherjee, S., "Recent advances in self-interference incoherent digital holography," Advances in Optics and Photonics 11(1), 1–66 (2019).
[9] Liu, J. P., Tahara, T., Hayasaki, Y. and Poon, T. C., "Incoherent Digital Holography: A Review," Appl. Sci. 8(1), 143 (2018).
[10] Tahara, T., Zhang, Y., Rosen, J. *et al*. "Roadmap of incoherent digital holography," Appl. Phys. B 128(11), 193 (2022).
[11] Rosen, J. and Brooker, G., "Digital spatially incoherent Fresnel holography," Opt. Lett. 32(8), 912-914 (2007).
[12] Brooker, G., Siegel, N., Wang, V. and Rosen, J., "Optimal resolution in Fresnel incoherent correlation holographic fluorescence microscopy," Opt. Express 19(6), 5047-5062 (2011).
[13] Vijayakumar A., Kashter Y., Kelner R. and Rosen J., "Coded aperture correlation holography–a new type of incoherent digital holograms," Opt. Express 24(11), 12430-12441 (2016).
[14] Vijayakumar A., Kashter Y., Kelner R. and Rosen J., "Coded aperture correlation holography system with improved performance [Invited]," Appl. Opt. 56(13), F67-F77 (2017).
[15] Ables, J. G., "Fourier transform photography: A new method for X-ray astronomy," Proc. Astron. Soc. Aust. 1(4), 172–173 (1968).
[16] Dicke, R. H., "Scatter-hole cameras for X-rays and gamma rays," Astrophysical Journal 153, L101 (1968).
[17] Fenimore, E. E. and Cannon, T. M., "Coded aperture imaging with uniformly redundant arrays," Appl. Opt. 17(3), 337-347 (1978).
[18] Chi, W. and George, N., "Optical imaging with phase-coded aperture," Opt. Express 19(5), 4294-4300 (2011).
[19] Horisaki, R., Ogura, Y., Aino, M. and Tanida, J., "Single-shot phase imaging with a coded aperture," Opt. Lett. 39(22), 6466-6469 (2014).
[20] Vijayakumar, A. and Rosen, J., "Interferenceless coded aperture correlation holography–a new technique for recording incoherent digital holograms without two-wave interference," Opt. Express 25(12), 13883-13896 (2017).
[21] Rai, M. R., Vijayakumar, A. and Rosen, J., "Non-linear adaptive three-dimensional imaging with interferenceless coded aperture correlation holography (I-COACH)," Opt. Express 26(14), 18143-18154 (2018).
[22] Bulbul, A., Hai, N. and Rosen, J., "Coded aperture correlation holography (COACH) with a superior lateral resolution of FINCH and axial resolution of conventional direct imaging systems," Opt. Express 29(25), 42106-42118 (2021).
[23] Smith, D., Gopinath, S., Arockiaraj, F. G., Reddy, A. N. K., Balasubramani, V., Kumar, R., Dubey, N., Ng, S. H., Katkus, T., Selva, S.J. *et al*. "Nonlinear Reconstruction of Images from Patterns Generated by Deterministic or Random Optical Masks—Concepts and Review of Research," J. Imaging 8(6), 174 (2022).
[24] Richardson, W. H., "Bayesian-Based Iterative Method of Image Restoration*," J. Opt. Soc. Am. 62(1), 55-59 (1972).
[25] Lucy, L. B., "An iterative technique for the rectification of observed distributions," The Astronomical Journal 79, 745 (1974).
[26] Anand, V., Han, M., Maksimovic, J., Ng, S. H., Katkus, T., Klein, A., Bambery, K., Tobin, M. J., Vongsvivut, J. and Juodkazis, S., "Single-shot mid-infrared incoherent holography using Lucy-Richardson-Rosen algorithm," Opto-Electron Sci. 1(3), 210006 (2022).
[27] Praveen, P. A., Arockiaraj, F. G., Gopinath, S., Smith, D., Kahro, T., Valdma, S. M., Bleahu, A., Ng, S. H., Reddy, A. N. K., Katkus, T. *et al*. "Deep Deconvolution of Object Information Modulated by a Refractive Lens Using Lucy-Richardson-Rosen Algorithm," Photonics 9(9), 625 (2022).
[28] Gopinath, S., Angamuthu, P. P., Kahro, T., Bleahu, A., Arockiaraj, F. G., Smith, D., Ng, S. H., Juodkazis, S., Kukli, K., Tamm, A. and Anand, V., "Implementation of a large-area diffractive lens using multiple sub-aperture diffractive lenses and computational reconstruction," Photonics 10(1), 3 (2022).
[29] Jayavel, A., Gopinath, S., Periyasamy Angamuthu, P., Arockiaraj, F. G., Bleahu, A., Xavier, A. P. I., Smith, D., Han, M., Slobozhan, I., Ng, S.H. *et al*. "Improved Classification of Blurred Images with Deep-Learning Networks Using Lucy-Richardson-Rosen Algorithm," Photonics 10(4), 396 (2023).
[30] Vijayakumar, A., "Tuning Axial Resolution Independent of Lateral Resolution in a Computational Imaging System Using Bessel Speckles," Micromachines 13(8), 1347 (2022).
[31] Kumar, R., Anand, V. and Rosen, J., "3D single shot lensless incoherent optical imaging using coded phase aperture system with point response of scattered airy beams," Sci. Rep 13(1), 2996 (2023).

[32] Bleahu, A., Gopinath, S., Kahro, T., Angamuthu, P. P., John Francis Rajeswary, A. S., Prabhakar, A., Kumar, R., Salla, G., Singh, R., Kukli, K., Tamm, A., Rosen, J. and Vijayakumar, A., "3D incoherent imaging using an ensemble of sparse self-rotating beams," Opt. Express 31(16), 26120-26134 (2023).
[33] Gerchberg, R. W., "A practical algorithm for the determination of plane from image and diffraction pictures," Optik, 35(2), 237-246 (1972).
[34] Gopinath, S., Bleahu, A., Kahro, T., John Francis Rajeswary, A. S., Kumar, R., Kukli, K., Tamm, A., Rosen, J. and Vijayakumar, A., "Enhanced design of multiplexed coded masks for Fresnel incoherent correlation holography," Sci. Rep. 13(1), 7390 (2023).